Available online at www.sciencedirect.com

ScienceDirect

Geochimica et Cosmochimica Acta 215 (2017) 92–104

Geochimica et Cosmochimica Acta

www.elsevier.com/locate/gca

U-series disequilibria of trachyandesites from minor volcanic centers in the Central Andes

Fang Huang [a,b,c,*], Erik V. Sørensen [d], Paul M. Holm [e], Zhao-Feng Zhang [f], Craig C. Lundstrom [b]

[a] CAS Key Laboratory of Crust-Mantle Materials and Environments, School of Earth and Space Sciences, USTC, Hefei 230026, China
[b] Department of Geology, University of Illinois at Urbana-Champaign, Urbana, IL 61801, USA
[c] Institute of Geochemistry and Petrology, ETH Zurich, CH-8092 Zurich, Switzerland
[d] Geological Survey of Denmark and Greenland, DK-1350 Copenhagen, Denmark
[e] Department of Geoscience and Natural Resource Management, University of Copenhagen, Dk-1350 Copenhagen, Denmark
[f] State Key Laboratory of Isotope Geochemistry, Guangzhou Institute of Geochemistry, CAS, Guangzhou 510640, China

Received 1 October 2015; accepted in revised form 11 July 2017; Available online 19 July 2017

Abstract

Young trachyandesite lavas from minor volcanic centers in the Central Andes record the magma differentiation processes at the base of the lower continental crust. Here we report U-series disequilibrium data for the historical lavas from the Andagua Valley in Southern Peru to define the time-scale and processes of magmatism from melting in the mantle wedge to differentiation in the crust. The Andagua lavas show (^{230}Th)/(^{238}U), (^{231}Pa)/(^{235}U), and (^{226}Ra)/(^{230}Th) above unity except for one more evolved lava with ^{230}Th depletion likely owing to fractional crystallization of accessory minerals. The ^{226}Ra excess indicates that the time elapsed since magma emplacement and differentiation in the deep crust is within 8000 years. Based on the correlations of U-series disequilibria with SiO_2 content and ratios of incompatible elements, we argue that the Andagua lavas were produced by mixing of fresh mantle-derived magma with felsic melt of earlier emplaced basalts in the deep crust. Because of the lack of sediment in the Chile-Peru trench, there is no direct link of recycled slabs with ^{230}Th and ^{231}Pa excesses in the Andagua lavas. Instead, ^{230}Th and ^{231}Pa excesses are better explained by in-growth melting in the upper mantle followed by magma differentiation in the crust. Such processes also produced the ^{226}Ra excess and the positive correlations among (^{226}Ra)/(^{230}Th), Sr/Th, and Ba/Th in the Andagua lavas. The time-scale of mantle wedge melting should be close to the half-life of ^{231}Pa (ca. 33 ka), while it takes less than a few thousand years for magma differentiation to form intermediate volcanic rocks at a convergent margin.

Keywords: U-series disequilibria; Magma differentiation; Central volcanic zone; Andes; Continental crust

1. INTRODUCTION

Subduction of the Nazca plate beneath the South American Plate since the mid-Oligocene has resulted in a thickened continental crust in the Andean orogenic belt (Mamani et al., 2010). This is a major tectono-magmatic zone of modern crustal growth as marked by numerous active volcanoes and giant caldera systems (Delph et al., 2017). Because the Andes Mountain belt is one of the largest subduction zones with a wide distribution of intermediate and silicic igneous rocks (Mamani et al., 2010), studies of Andean magmatism shed light on intra-crustal differentiation processes and crustal growth at convergent margins.

* Corresponding author at: CAS Key Laboratory of Crust-Mantle Materials and Environments, School of Earth and Space Sciences, USTC, Hefei 230026, China.
E-mail address: fhuang@ustc.edu.cn (F. Huang).

http://dx.doi.org/10.1016/j.gca.2017.07.017
0016-7037/

Multiple models, such as MASH (mixing, assimilation, storage and homogenization), AFC (assimilation and fractional crystallization), and magma mixing, have been proposed to address how the evolved igneous rocks in the Andes formed (e.g. DePaolo, 1981; Hildreth and Moorbath, 1988; Sørensen and Holm, 2008). Although recent seismic imaging studies (Delph et al., 2017) show areas of low seismic velocity at the crust-mantle transition which is interpreted as a MASH zone in the plumbing system beneath the thick continental crust in the Central Volcanic Zone (CVZ) (Delph et al., 2017), the processes and time-scales of mantle melting and magmatism in a cordilleran system are still not well understood.

U-series disequilibria provide a unique tool to constrain the magmatic processes at convergent margins because radioactive disequilibria between U-series parent-daughter nuclides will return to secular equilibrium after 5 times the half-life of the daughter (e.g. Bourdon and Sims, 2003; Lundstrom, 2003; Turner et al., 2003 and references therein). Most young subduction zone lavas have (^{226}Ra)/(^{230}Th) and (^{231}Pa)/(^{235}U) (the parentheses stand for radioactivity ratio) greater than unity. While the majority of young lavas have excesses of ^{238}U over ^{230}Th, ^{230}Th excesses over ^{238}U are also observed in a substantial number of samples (e.g. Bourdon et al., 1999; Turner et al., 2000; Sigmarsson et al., 2002; Thomas et al., 2002; Bourdon et al., 2003; Dosseto et al., 2003; George et al., 2003; Turner et al., 2003; Reagan et al., 2008; Huang et al., 2011, 2016; Reubi et al., 2011; Avanzinelli et al., 2012).

The generation and temporal implications of U-series disequilibria in subduction zone lavas are still debated. It has been suggested that U-series disequilibria observed in subduction zone lavas could be inherited from the mantle source modified by flux from the subducted slab (such as via hydrous fluid or sediment melt) (e.g. Bourdon et al., 2003; Turner et al., 2003; Avanzinelli et al., 2012). If so, the time-scale from subducted material addition to the mantle wedge to magma eruption should be within five half-lives of the daughter nuclide of each parent daughter pair (e.g. Turner et al., 2001). However, it has also been recently proposed that in-growth melting in the mantle wedge could produce U-series disequilibria in subduction zone lavas (Huang et al., 2011, 2016; Reubi et al., 2011). In this view, the U-series disequilibrium signatures in convergent margin magmas reflect a series of processes including metasomatism and partial melting of the mantle wedge followed by magma ascent in the mantle and time-dependent differentiation in the crust. In particular, assessing variations in U-series disequilibria with magmatic differentiation indices (such as SiO_2) provides an effective method to distinguish source signatures from those developed during magma differentiation processes (Huang et al., 2016).

The CVZ of the Andes has a ~ 70 km thick crust with a geographically wide distribution of volcanoes from the Pleistocene to Recent (Bourdon et al., 2000; Delacour et al., 2007; Mamani et al., 2010). Among these volcanoes, the large stratovolcanoes making up the bulk of the CVZ typically contain plagioclase and amphibole-bearing porphyritic rocks which mainly reflect modification during differentiation at shallow crustal levels (DePaolo, 1981; Hildreth and Moorbath, 1988; Mamani et al., 2010). In contrast, lavas from some minor volcanoes were suggested to be tapped from magma chambers in the deep crust (Delph et al., 2017) and thus they have been used to "see through" the magma differentiation that is typically observed in lavas from stratovolcanoes (Davidson and de Silva, 1992). Such minor centers are often located behind the main arc and their distribution appears controlled by structural lineaments within the crust. The volcanic cones are typically 200–300 meters high with diameters of 500–650 meters (Delacour et al., 2007). Because they have erupted chemically less evolved lavas than the major stratovolcanoes (Delph et al., 2017), the primary signals (such as high Sr/Y) of magma differentiation at the base of the lower crust are better preserved without much stagnation and modification in the shallow depths (Davidson and de Silva 1992; Mattioli et al., 2006; Delacour et al., 2007; Sørensen and Holm, 2008). For instance, it has been proposed that major and trace element compositions of lavas from minor volcanoes around Andagua in Southern Peru mainly reflect signatures of magma mixing in the deep crust (Sørensen and Holm, 2008).

Because magma differentiation in the upper crust could obscure the primary U-series disequilibria and other geochemical features of subduction zone magmas (e.g. Huang et al., 2008, 2011; Reubi et al., 2011), young lavas from the minor volcanoes are better candidates for the U-series study of magmatic processes in the deep crust. The occurrence in the CVZ of minor volcanoes provides an excellent opportunity to address the time-scales and processes of mantle-derived magma evolution in the deep crust. Therefore, we here present U-Th-Pa-Ra data for a suite of well-characterized historical trachyandesites from the Andagua Valley, S. Peru (Fig. 1). The purpose of this study is to provide insights into the intrinsic relationships among mantle melting, magma differentiation, and crustal growth in the continental subduction zone. We find that the Andagua lavas have significant U-series disequilibria, which place critical temporal constraints on melting in the mantle wedge and magma differentiation processes in the crust.

2. GEOLOGICAL SETTING AND SAMPLE DESCRIPTIONS

The Andean orogenic belt forms a continuous mountain chain over a length of >7500 km, resulting from subduction of the Nazca Plate under the South American Plate (e.g. Harmon et al., 1984; Hildreth and Moorbath, 1988; Stern, 2004; Sørensen and Holm, 2008; Mamani et al., 2010). It is segmented into the Northern Volcanic zone, the CVZ, and the Southern Volcanic zone. The CVZ is between 14°S and 28°S and has the thickest continental crust of all global subduction zones, a feature that has been related to tectonic shortening in the last 30 Ma (Baby et al., 1997). Seismic studies of the thermo-mechanical properties of the crust indicate that the upper 50 km of the crust is felsic while the lower part is mafic (Yuan et al., 2002).

The Andagua valley (15 °32′ S, 72 °19′ W) is located in the northernmost part of the CVZ (southern Peru) and is

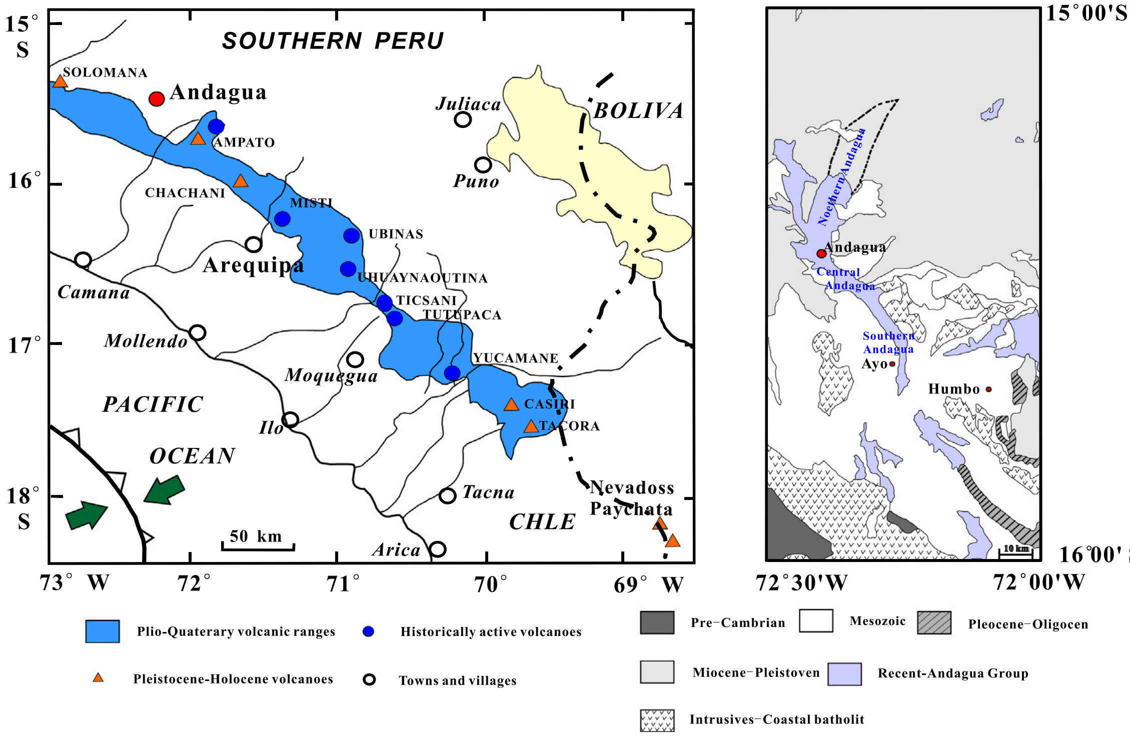

Fig. 1. Geological map for the Central Volcanic Zone and Andagua lavas modified from Sørensen and Holm (2008).

~230 km inboard of the Peru–Chile trench, situated ~125 km above the Benioff zone of the subducting slab (Fig. 1) (Sørensen and Holm, 2008). The valley is characterized by abundant volcanic features (scoria cones, lava flows, and domes) that belong to the more widespread quaternary Andahua Group (Caldas, 1993; Gałaś, 2011, 2014). Here, we focus on some of the youngest historical lavas (Chilcayoc Grande, Chilcayoc Chico 1, Chilcayoc Chico 2, Jenchana, Ninamama, Ninacaca, Jechapita, and Sucna 1) found in the lower part of the valley, southeast of the Andagua village described in Sørensen and Holm (2008). Although the ages of the volcanoes are not well constrained, a ^{14}C age determination yields 370 ± 50 BP for the organic materials captured in lavas from Chilcayoc Chico 1 was reported in Cabrera and Thouret (2000), indicating that the lavas are young.

Based on detailed field, petrographic, and geochemical study of the Andagua lavas, Sørensen and Holm (2008) revealed that binary mixing between compositionally different parental magmas combined with subsequent fractional crystallization in the deep crust explains the compositional variability observed in the youngest lavas. Key observations include high Sr/Y and low Y contents and positive correlations between Rb and Sr (being both incompatible) within co-magmatic groups coupled to overall negative correlations for Rb-Sr between the co-magmatic groups. This suggests that the binary mixing took place at high pressure within the stability field of garnet (instead of plagioclase).

3. ANALYTICAL METHODS

Seventeen trachyandesite samples with a range of SiO_2 from 55 to 60 wt.% and high Na_2O contents (4.2–5.2 wt.%) were selected for U-series disequilibria analyses. Additionally, two samples from the Puca Mauras complex north of Andagua (probably older than 10,000 yrs (Gałaś, 2014)) and one sample from Ninacaca were also selected to examine the U-series data in more evolved SiO_2-rich samples. More details on samples are available in Sørensen and Holm (2008). U-series disequilibria of the Andagua samples were measured using isotope dilution methods on the Nu-Instrument MC-ICP-MS in the Department of Geology at University of Illinois at Urbana-Champaign (UIUC) following the procedures described in Huang and Lundstrom (2007) and Huang et al. (2011). U, Th, Pa, and Ra concentrations were measured by the isotope dilution method using high purity artificial ^{236}U, ^{229}Th, ^{233}Pa, and ^{228}Ra. The content of ^{228}Ra tracer was calibrated by mixing and measurement with BCR-2 assuming that it has $(^{226}Ra)/(^{230}Th) = 1.00$. Protactinium separation followed the procedures described in Regelous et al. (2004). Briefly, protactinium was separated from high field strength elements and other interferences using AG1-X8 100–200 mesh and TRU spec 50–100 mesh resins. U and Th were separated using anion-resin columns, and Ra was purified from Th and Ba using a cation resin column followed by a Sr-Spec resin column. The procedural blanks of U-Th-Pa-Ra are negligible relative to the amounts of U-series nuclides of samples (Huang et al., 2011).

Rock standards BCR-2 and ATHO-1 were measured to validate the accuracy and precision of U-series measurement in the UIUC isotope laboratory (Table 1) (Huang and Lundstrom, 2007; Huang et al., 2011). U-Th-Pa-Ra concentrations and U-series data of these two standards are within error of recommended literature values (Prytulak et al., 2008; Sims et al., 2008; Koornneef et al.,

Table 1
U-series disequilibrium data and Gd/Yb of Andagua samples and standards.

Sample	Area	Subarea	Volcanic unit	U (ppm)	Th (ppm)	(^{230}Th)/(^{232}Th)	(^{238}U)/(^{232}Th)	(^{230}Th)/(^{238}U)	(^{234}U)/(^{238}U)	^{231}Pa (fg/g)	(^{231}Pa)/(^{235}U)	^{226}Ra (fg/g)	(^{226}Ra)/(^{230}Th)	Gd/Yb
121-005	Central Andagua	Jenchana	Jenchana	0.585	2.859	0.67	0.620	1.08	1.00	298	1.57	245	1.15	5.38
121-007			Jenchana	0.582	2.842	0.67	0.621	1.08	1.00	292	1.54	233	1.10	5.44
121-043			Jenchana	0.573	2.864	0.66	0.607	1.08	1.00	294	1.58	237	1.13	5.54
Duplicate				0.571	2.862	0.67	0.605	1.10	1.00	277	1.49	238	1.12	
Average				0.572	2.863	0.66	0.606	1.09	1.00	285	1.53	238	1.13	
121-076			Jenchana	0.580	2.827	0.67	0.622	1.07	1.00	291	1.54	249	1.11	5.44
121-011	Central Andagua	Chilcayoc Chico 1	Chilcayoc Chico 1	0.629	3.068	0.70	0.621	1.13	1.00	316	1.55	266	1.11	5.32
Duplicate				0.635	3.109	0.70	0.620	1.13	1.00	321	1.55	270	1.11	
Average				0.632	3.089	0.70	0.621	1.13	1.00	318	1.55	268	1.11	
121-013			Chilcayoc Chico 1	0.659	3.311	0.75	0.604	1.23	1.00	348	1.62	317	1.15	4.79
121-141			Chilcayoc Chico 1	0.668	3.298	0.76	0.614	1.23	1.00	352	1.62	304	1.09	4.57
Duplicate				0.667	3.295	0.76	0.614	1.23	1.00	350	1.61			
Average				0.667	3.297	0.76	0.614	1.23	1.00	351	1.62	304	1.09	
121-034	Central Andagua	Ninamama	U-lava	0.825	3.883	0.73	0.644	1.14	1.00	403	1.50	322	1.01	4.10
Duplicate				0.825	3.880	0.72	0.645	1.11	1.00	392	1.46	312	1.00	
Average				0.825	3.881	0.73	0.644	1.13	1.00	398	1.48	317	1.01	
121-039			Ninamama	0.673	3.366	0.69	0.606	1.14	1.00	346	1.58	282	1.09	4.06
121-051			Ninamama	0.812	3.877	0.73	0.635	1.15	1.00	394	1.49	330	1.05	4.12
121-055	Central Andagua	Ninacaca	Ninacaca	0.941	5.639	0.53	0.506	1.05	1.00	398	1.30	340	1.02	4.83
121-085	Central Andagua	Chilcayoc Chico 2	Chilcayoc Chico 2	0.550	2.706	0.66	0.617	1.07	1.00	274	1.53	241	1.21	5.30
121-089	Central Andagua	Sucna 1	Sucna 1	0.585	2.889	0.69	0.614	1.12	1.00	312	1.64	251	1.13	5.06
121-107			Sucna 1	0.583	2.931	0.67	0.603	1.11	1.00	302	1.59	248	1.14	5.10
Duplicate				0.583	2.939	0.67	0.601	1.12	1.00	308	1.63	245	1.11	
Average				0.583	2.935	0.67	0.602	1.11	1.00	305	1.61	246	1.12	
121-121	Central Andagua	Chilcayoc Grande	Chilcayoc Grande	0.532	2.472	0.68	0.652	1.04	1.00	251	1.45	215	1.15	5.81
121-122			Chilcayoc Grande	0.476	2.219	0.72	0.651	1.11	1.00	215	1.39	216	1.21	5.35
121-137			Chilcayoc Grande	0.428	1.753	0.75	0.740	1.00	1.00	197	1.41	189	1.31	5.72
Duplicate				0.426	1.719		0.752		1.01			189		
Average				0.427	1.736	0.75	0.746	1.00	1.01	197	1.41	189	1.31	
121-143			Chilcayoc Grande	0.537	2.475	0.70	0.658	1.06	1.00	266	1.52	215	1.12	5.57
121-061	North Andagua	Puca Mauras	Puca Mauras 3	0.897	5.952	0.47	0.457	1.04	1.00	321	1.10	308	0.98	5.42
121-130			Puca Mauras 4	2.069	5.676	0.95	1.106	0.86	1.00	696	1.03	584	0.98	4.35
Duplicate				2.061	5.635	0.94	1.109	0.85	1.00					
Average				2.065	5.655	0.94	1.107	0.85	1.00	696	1.03	584	0.98	
BCR-2				1.697	5.879	0.88	0.875	1.00	1.00	552	1.00	576	1.00	
2stdev				0.004	0.026	0.01	0.005	0.02	0.01	17	0.03	13	0.03	

(*continued on next page*)

Table 1 (*continued*)

Sample	Area	Subarea	Volcanic unit	U (ppm)	Th (ppm)	$(^{230}Th)/(^{232}Th)$	$(^{238}U)/(^{232}Th)$	$(^{230}Th)/(^{238}U)$	$(^{234}U)/(^{238}U)$	^{231}Pa (fg/g)	$(^{231}Pa)/(^{235}U)$	^{226}Ra (fg/g)	$(^{226}Ra)/(^{230}Th)$	Gd/Yb
BCR-2*				1.696	5.907	0.87	0.870	1.00	1.00	551	1.00			
2stdev				0.003	0.001	0.01	0.000	0.00	0.00	28	0.05			
ATHO*				2.234	7.471	0.91	0.906	1.14	1.00			854	1.13	
2stdev				0.024	0.033	0.69	0.090	1.12	0.01			29	1.14	

BCR-2 data are based on the average of three analyses for U-Th-Pa-Ra.

* Data are from Huang et al. (2011), which were measured in the Department of Geology, University of Illinois at Urbana-Champaign.

2010), suggesting the reliability of our analyses. Three analyses of BCR-2 indicate that the reproducibility for U and Th concentrations are smaller than 0.5%, Ra and Pa smaller than 3% (2σ). The in-run analytical uncertainties are significantly smaller than the reproducibility of standard analyses. Duplicated measurements were performed for eight out of the twenty samples, and the results also show excellent reproducibility (Table 1).

4. RESULTS

U-series data of the Andagua Valley lavas are shown in Table 1 and Fig. 2. Although the eruption ages of the lavas are not well-known, most of the samples have ^{226}Ra excess with $(^{226}Ra)/(^{230}Th)$ ranging from 1.04 to 1.31 (Table 1, Fig. 2), suggesting that the age of most samples is <8000 years and thus the effect of ageing since eruption on $(^{238}U)/(^{230}Th)$ and $(^{231}Pa)/(^{235}U)$ is negligible. Therefore, age corrections were not performed for ^{230}Th-^{238}U and ^{231}Pa-^{235}U data. $(^{234}U)/(^{238}U)$ of all samples are within analytical error of unity (<3% based on duplicated analysis of ATHO in Huang et al. (2011)), indicating that weathering or alteration after eruption (if any) did not significantly change U-series disequilibrium data of the Andagua samples.

U and Th contents of the Central Andagua samples show significant variations from 0.43 to 0.94 ppm and 1.74 to 5.64 ppm, respectively (Fig. 3a and b), and both are positively correlated with SiO_2 content (Fig. 3c). $(^{238}U)/(^{232}Th)$ ranges from 0.601 to 0.746, except for two more evolved samples from Puca Mauras (121-061 and 121-130) which have high SiO_2 content and are likely older than 10,000 years (Sørensen and Holm, 2008; Gałaś, 2014). These two samples also have highest U-Th contents and largest difference in $(^{238}U)/(^{232}Th)$. Sample 121-130 has the highest $(^{238}U)/(^{232}Th)$ (1.107) and sample 121-061 has the lowest (0.457) among all the Andagua lavas. Furthermore, the three high-SiO_2 samples from Puca Mauras and Ninacaca all have lower $(^{230}Th)/(^{238}U)$, $(^{231}Pa)/(^{235}U)$, and $(^{226}Ra)/(^{230}Th)$ relative to the lavas with lower SiO_2 contents (Fig. 4a –c). Notably, sample 121-130 is the only sample with a ^{230}Th deficit, likely due to the effect of accessory mineral crystallization (see discussion below). If these three samples are excluded, all Andagua lavas have $(^{230}Th)/(^{238}U)$ and $(^{226}Ra)/(^{230}Th)$ ranging from unity to 1.23 and 1.31, respectively, and $(^{231}Pa)/(^{235}U)$ from 1.39 to 1.64. Overall, $(^{230}Th)/(^{238}U)$ and $(^{231}Pa)/(^{235}U)$ of the Andagua lavas show roughly positive correlations with SiO_2 contents, while $(^{226}Ra)/(^{230}Th)$ is negatively correlated with SiO_2. There is also a rough positive correlation between $(^{230}Th)/(^{238}U)$ and $(^{231}Pa)/(^{235}U)$ (Fig. 2b). No clear correlation between U-series disequilibrium data and SiO_2 content is observed in lavas from individual volcanic units (Fig. 3).

5. DISCUSSION

5.1. Effect of magma differentiation on U-series disequilibria

As recent studies have pointed out, most subduction zone lavas have experienced significant extents of differenti-

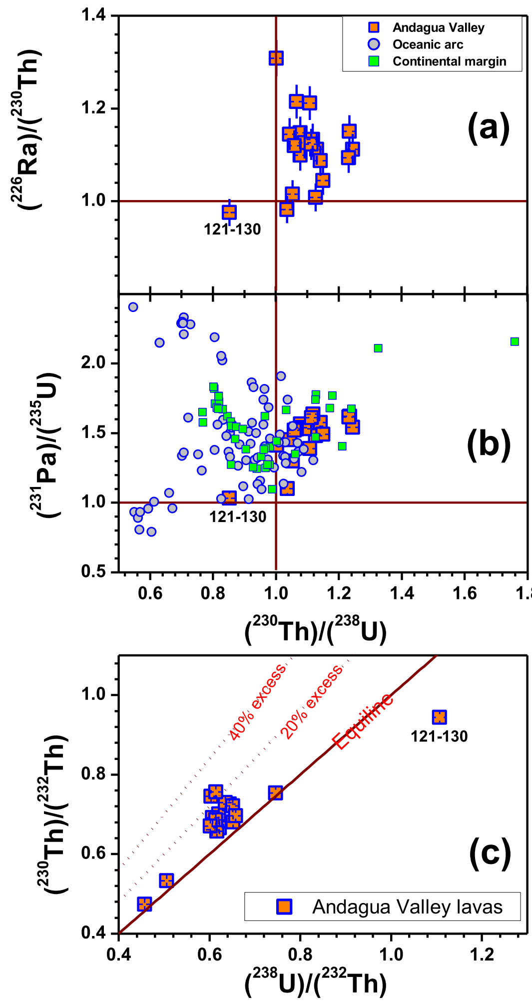

Fig. 2. Comparison of U-series disequilibria of lavas from the Andagua valley with those from oceanic arcs and continental margin. Most Andagua samples have ^{226}Ra, ^{230}Th, and ^{231}Pa excesses, while sample 121-130 has ^{230}Th deficit likely due to fractional crystallization of allanite and apatite. Data sources of Fig. 2b: Asmerom et al. (2005), Bourdon et al. (1999), Dosseto et al. (2003), Huang and Lundstrom (2007), Pickett and Murrell (1997), Reubi et al. (2011, 2014), Thomas et al. (2002), Turner et al. (2006), Zellmer et al. (2003), Huang et al. (2011), and Avanzinelli et al. (2012).

ation, meaning that U-series data of subduction zone lavas could have been modified by magma mixing, assimilation of wall rocks, ageing, crystallization, and recharge of fresh melt (Huang et al., 2008; Huang et al., 2011; Reubi et al., 2011; Huang et al., 2016). Because the decay of ^{231}Pa-^{235}U and ^{230}Th-^{238}U after eruption is negligible as indicated by the existence of significant ^{226}Ra excess, the U-series data of these samples can be directly applied without age correction to model magmatic processes, including mantle melting and crustal magma differentiation.

The three samples from Puca Mauras and Ninacaca have large variations in U/Th, with clear evidence for magma differentiation, such as the high SiO_2 content (>60 wt.%). The two lavas from Puca Mauras have high

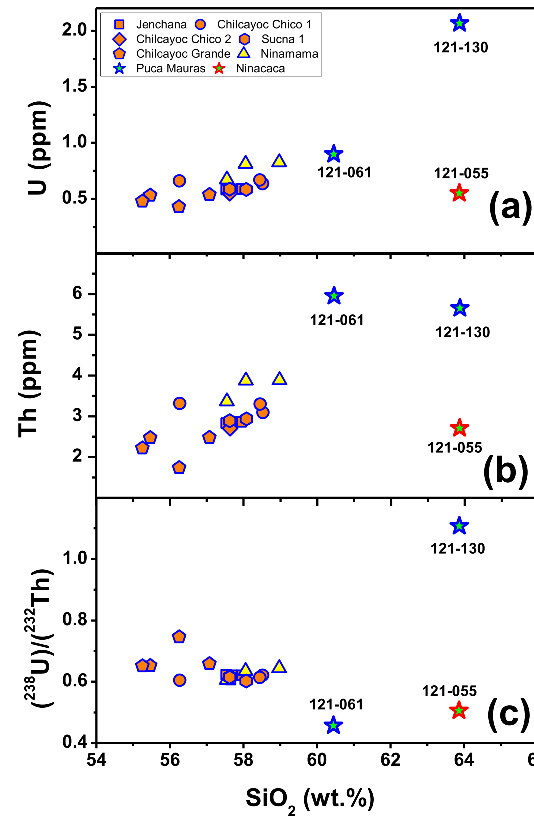

Fig. 3. Correlation of SiO_2 with U, Th, and (^{238}U)/(^{230}Th) for the Andagua lavas. U and Th contents of the Andagua lavas increase with SiO_2 content. (^{238}U)/(^{232}Th) does not obviously change with SiO_2, while the three more differentiated samples show a large variation in (^{238}U)/(^{232}Th).

U-Th contents (Fig. 3a and b) and they also have low ^{231}Pa excess and (^{226}Ra)/(^{230}Th) within error of unity (Fig. 4), consistent with their older eruption ages relative to other samples. The high SiO_2 contents, large variations in U/Th ratios, and U-series disequilibria of Puca Mauras lavas likely reflect the effects of ageing and fractional crystallization of accessory minerals during magma evolution because fractionating accessory minerals (such as apatite, allanite, and zircon) can dramatically change Th/U in the high SiO_2 melt (Hermann, 2002; Blundy and Wood, 2003; Garrison et al., 2006; Prowatke and Klemme, 2006). For instance, an experimental study on partitioning of trace elements between allanite and hydrous granitic melts at 2 GPa and 900 °C shows that $^{allanite/melt}D_{Th}$ is 60, $^{allanite/melt}D_{Th/U}$ is 3, and $^{allanite/melt}D_{Ce/Th}$ is ~3 (Hermann, 2002). Therefore, the lower (^{230}Th)/(^{238}U) and Ce content in sample 121-130 compared to the other Andagua samples could be explained by crystallizing allanite as an accessory mineral which can preferentially remove Th and Ce relative to U from more evolved magmas (Garrison et al., 2006). Because U is more compatible than Th in zircon, sample 121-055 and 121-061 have low U/Th and high (^{230}Th)/(^{238}U) in Figs. 4b and 5a, likely reflecting crystallizing zircon and ageing effect as indicated by the lower (^{226}Ra)/(^{230}Th) and ^{231}Pa excess relative to the less evolved lavas.

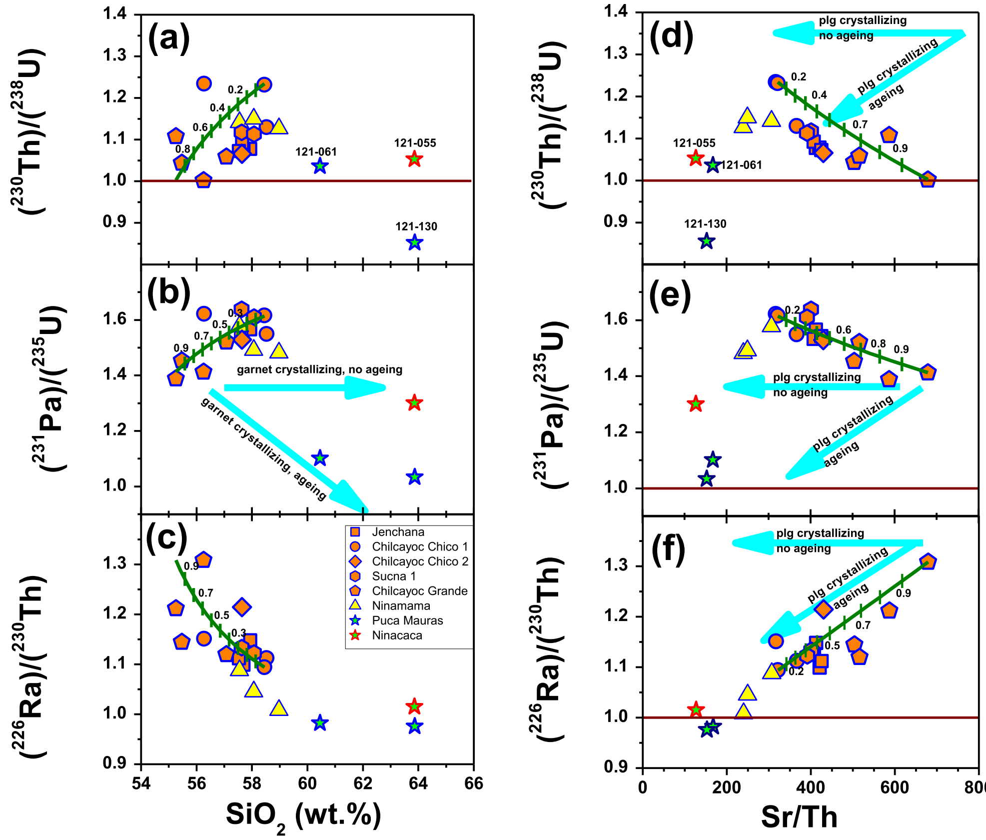

Fig. 4. The correlations of SiO_2 and Sr/Th with U-series disequilibria of the Andagua lavas suggest magma mixing processes in the deep crust. Except the three more differentiated samples and three Ninamama samples with different mineralogy and origins (Sørensen and Holm, 2008), SiO_2 is positively correlated with $(^{230}Th)/(^{238}U)$ (a) and $(^{231}Pa)/(^{235}U)$ (b), but negatively with $(^{226}Ra)/(^{230}Th)$ (c), while Sr/Th is negatively correlated with $(^{230}Th)/(^{238}U)$ (d) and $(^{231}Pa)/(^{235}U)$ (e), but positively with $(^{226}Ra)/(^{230}Th)$ (f). These correlations can be explained by mixing between mafic and felsic magmas. The light blue arrows denote the effect of crystallizing plagioclase (plg) and garnet with or without ageing effect. SiO_2 and Sr contents are from Sørensen and Holm (2008). The numbers close to the mixing curve represent fractions of mafic end-member. Parameters used in the mixing models are listed in Table 2.

5.2. Constraints on magma differentiation in the deep crust

The Quaternary intermediate igneous rocks in the CVZ are characterized by high Sr/Y, La/Yb, and Gd/Yb which are considered signatures produced by garnet as a residual phase during magmatism. This is important because garnet (in contrast to other mafic minerals such as clinopyroxene and amphibole) is critical for fractionating U-series nuclides and heavy rare earth elements during crustal magmatism (Salters and Longhi, 1999; Pertermann et al., 2004; Delacour et al., 2007; Sørensen and Holm, 2008; Mamani et al., 2010). Because the subducting Nazca plate is too old (44–60 Ma) and cold to melt even during flat subduction, the garnet signatures cannot be produced by slab melting. Instead, because high Sr/Y has been observed to be associated with increasing crustal thickness of the Central Andes (Mamani et al., 2010), we suggest that it is differentiation of magma in the extremely thick crust which imposes significant effects on the geochemical composition of the CVZ lavas.

5.2.1. The effect of fractional crystallization

Fractional crystallization of potentially important minerals is incapable of producing the observed variations in U-series disequilibria and other geochemical signatures of the Andagua lavas. Because crystallizing garnet increases the SiO_2 content of the melt, and because U and Pa are highly incompatible in garnet (e.g. Salters and Longhi, 1999; Blundy and Wood, 2003; Pertermann et al., 2004), solely fractional crystallization of garnet (with or without ageing effect) cannot explain the positive correlation between SiO_2 and $(^{231}Pa)/(^{235}U)$ (Fig. 4b). Furthermore, because fractionation of garnet increases Gd/Yb in the melt, and the ageing effect decreases ^{230}Th-^{238}U disequilibrium, the combination of such two effects could produce a negative correlation between Gd/Yb and $(^{230}Th)/(^{238}U)$. However, the direction of such effect is opposite to the trend of SiO_2 variation (Fig. 5b). Similarly, the negative correlations of Sr/Th with $(^{230}Th)/(^{238}U)$ and $(^{231}Pa)/(^{235}U)$ preclude the effects of plagioclase crystallizing and ageing because they would produce positive correlations among these parameters (Figs. 4e and 4d). Finally, fractionation of plagioclase at the upper crustal level cannot change Gd/Yb, $(^{230}Th)/(^{238}U)$, or $(^{231}Pa)/(^{235}U)$ in the melts because rare earth elements and U-Th-Pa are highly incompatible in plagioclase (Blundy and Wood, 2003; Zajacz and Halter, 2007) (Fig. 5). Consequently, the trachyandesites cannot be explained by

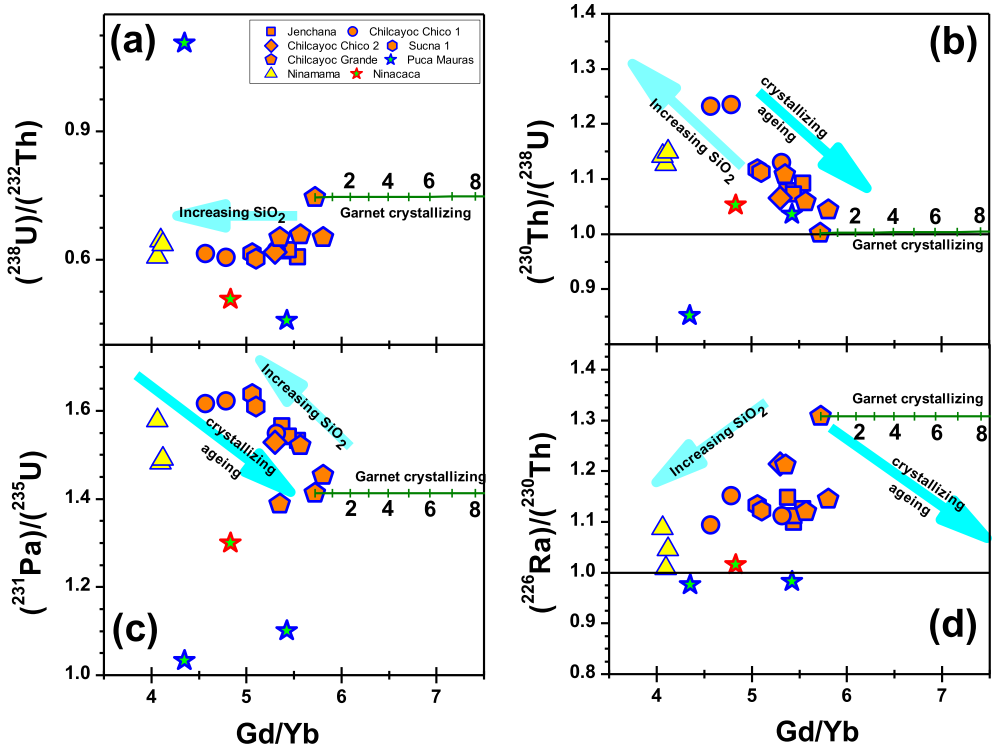

Fig. 5. Gd/Yd vs. U-series data of the Andagua lavas. Because Gd/Yb is not sensitive to plagioclase crystallization during shallow storage, it provides a good indicator for the deep crustal process in garnet-stability field. When the three more differentiated samples (marked in asteroid) and Ninamama samples (up-triangle) with contrasting origin to the rest of Andagua lavas are not included, (^{238}U)/(^{232}Th) does not significantly change with Gd/Yb, while (^{230}Th)/(^{238}U) is negatively correlated with Gd/Yb. Fractional crystallization of garnet increases Gd/Yb, but cannot produce the variations in U-series disequilibria. Instead, the variation of (^{230}Th)/(^{238}U) is more likely due to magma mixing. Gd and Yb data are from Table 1. Partition coefficients of Gd and Yb are 6.25 and 9.34, respectively, based on experiment MP254 in Pertermann et al. (2004). The numbers close to the model denote the proportion of garnet crystallization in percent.

fractional crystallization of mafic minerals or plagioclase from basaltic melt.

5.2.2. Magma mixing in the deep crust

Based on the discussion above, we propose that the Andagua trachyandesites were most likely produced by mixing between basaltic and felsic magmas in the deep crust at pressure >1.5 GPa. Such magmatic mixing may induce variations in Sr-Nd-Pb isotopic composition of the resulting magma (e.g. Hildreth and Moorbath, 1988; Sørensen and Holm, 2008), whereas U-series disequilibria of the Andagua lavas can show the sequence of multiple emplacement of mantle-derived magmas.

Although the composition of the lower crust of the CVZ is not well understood, we can still constrain the geochemical properties and origin of the mixing end-members based on U-series disequilibrium and other geochemical data. Given that the Andagua lavas have lower Mg# and MgO content than primitive basalts, the mafic end-member is likely differentiates of mantle-derived basalts recently emplaced into the crust within a few half-lives of ^{226}Ra. The Andagua lavas with higher SiO_2 content generally have lower Sr/Th and ^{226}Ra excess but greater ^{231}Pa and ^{230}Th excesses (Fig. 4). Because U is highly incompatible in garnet and clinopyroxene (Blundy and Wood, 2003), simple batch or fractional melting of old mafic rocks can only produce slight ^{231}Pa excess relative to ^{235}U. Incongruent in-growth dehydration melting of amphibolite in the crust could also produce U-series disequilibria in the resultant felsic melt if melting rates are lower than 10^{-2} kg/m^3 yr (Dufek and Cooper, 2005). However, such process would produce high ^{226}Ra excess (greater than 300%) (Dufek and Cooper, 2005), which is inconsistent with our observations that the felsic endmember should have low ^{226}Ra excess. Given the (^{231}Pa)/(^{235}U) up to 1.6 and slight ^{226}Ra excess in the felsic lavas, the felsic end-members is more likely to result from melting of earlier emplaced basalts (likely within a few half-lives of ^{226}Ra) in the deep crust, suggesting a scenario recently proposed in Barboni et al. (2016) that the arc magmas are stored in hot country rock of the chambers.

A model is thus used to quantify the mixing process. We use sample 121-141 from Chilcayoc Chico 1 to represent the felsic end-member and Chilcayoc Grande lavas (with the lowest SiO_2 among the Andagua lavas) to represent the mafic end-member (Table 2). Although end-members can only be roughly estimated for the moment, the mixing fractions of end-members could still be robust because the real mafic (or felsic) end-member should have lower (or high SiO_2) than the one used in the modelling. Nonetheless, the correlations between U-series disequilibria and other geochemical data (such as SiO_2 and Sr/Th) are self-consistently explained (Fig. 4). Furthermore, Sr/Th shows good positive correlations with Ba/Th and 1/Th, whereas Ba/Th is negatively correlated with SiO_2 content (Fig. 6),

Table 2
SiO_2 (wt.%), trace elements (ppm), and U-series disequilibrium data used in the mixing models.

End member	SiO_2	Sr	Ba	Th	U	$(^{230}Th)/(^{238}U)$	$(^{231}Pa)/(^{235}U)$	$(^{226}Ra)/(^{230}Th)$
Felsic	58.45	1061	1301	3.297	0.667	1.234	1.614	1.094
Mafic	55.26	1180	1038	1.736	0.427	1.002	1.413	1.308

Note: Mafic end-member parameters are based on sample 121-137 (Chilcayoc Grande) except SiO_2 from 121-122 (Chilcayoc Grande); felsic end-member parameters are based on sample 121-141 (Chilcayoc Chico 1).

which also supports that the Andagua lavas formed by magma mixing in the deep continental crust where plagioclase may not be the stable phase to affect Sr. Thus, this is consistent with mixing between the mafic and felsic magmas (Fig. 6).

Fig. 7 shows a conceptual sketch of the large scale plumbing system based on the seismic imaging of Delph et al. (2017). In our model, partial melting of convective metasomatized sub-arc mantle produces hydrous basaltic melt, which ascends to a MASH zone near the MOHO at the depths of about 70 km (Fig. 7a). In case of a typical stratovolcano, mantle-derived magma may have experienced significant differentiation in the MASH zone and also along the ascending route toward the Earth's surface before eruption, which in some cases do not always show high pressure signatures (such as high Sm/Yb) developed in the deep MASH zone (Mamani et al., 2010). On the contrary, for the minor volcanic centers in the Andagua valley, magma ascended through the crust without much stagnation in middle to upper crustal level magma chambers whereby signatures of the deep magma mixing got preserved. This is supported by the good correlations between U-series disequilibria and SiO_2 (or Gd/Yb and Sr/Th) of the Andagua lavas (Fig. 4 and Fig. 5). These show that any subsequent shallow differentiation did not change Gd/Yb and Sr/Th and the variation of these ratios reflect the heterogeneity of the mixing end-members. Furthermore, the U-series disequilibria of the Andagua lavas suggest that a younger mafic magma mixed with felsic melt likely derived from old basalts emplaced slightly earlier (Fig. 7b). Particularly, ^{226}Ra excess over ^{230}Th constrains that the time-scales from the mixing to magma ascent and final eruption should be within a few millennia. In summary, because understanding formation of intermediate rocks is a key for studying accretion and evolution of the continental crust (e.g. Gill, 1981; Grove and Kinzler, 1986), the data here provide important insight into the role of magma mixing in forming intermediate lavas and crustal growth in the continental subduction zones.

5.3. Implications for generating U-series disequilibria in subduction zone lavas

Debates on generation of U-series disequilibria in subduction zone lavas focus on whether they are inherited from subducted sediments (via hydrous fluid or sediment melt) (e.g. Bourdon et al., 2003; Turner et al., 2003; Avanzinelli et al., 2012) or produced by in-growth melting of the mantle wedge (Huang et al., 2016). Three lines of evidence suggest that recent addition of sediment melt to the wedge cannot explain the U-series disequilibria of the Andagua lavas. Firstly, there is no obvious accretion of sediments (if any) in the Chile-Peru trench as indicated by geophysical and ocean floor imaging studies (Thornburg and Kulm, 1987);

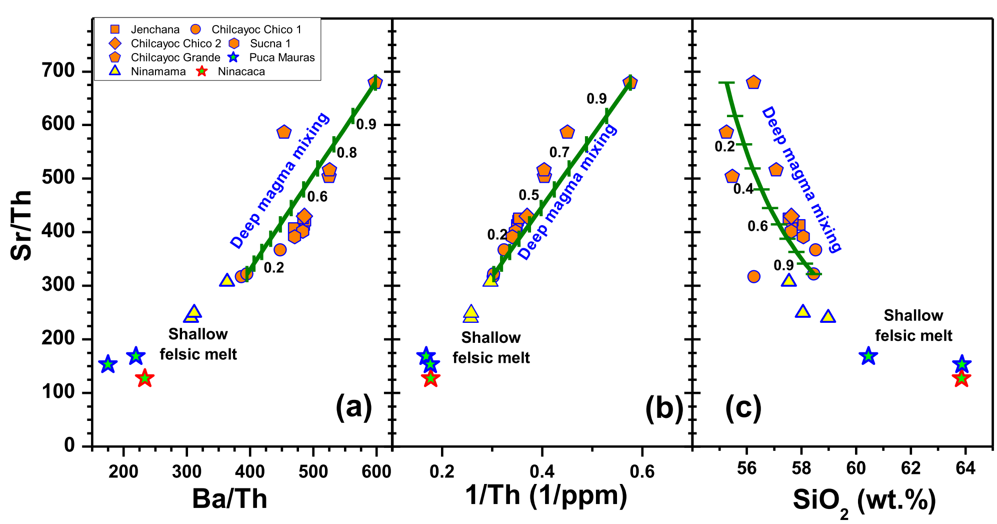

Fig. 6. Correlations of Sr/Th with Ba/Th, 1/Th, and SiO_2 of the Andagua lavas. Sr/Th is positively correlated with Ba/Th and 1/Th, but negatively with SiO_2. The large variation of Ba/Th and Sr/Th cannot be explained by fractional crystallization of minerals where Ba and Sr are more compatible than Th, such as plagioclase. Instead, it is more likely due to magma mixing between mafic and felsic end-members, which is also supported by other geochemical observations such as SiO_2 (see the main context for details). The numbers close to the mixing curve represent fraction of mafic end-member. Parameters used in the mixing models are listed in Table 2.

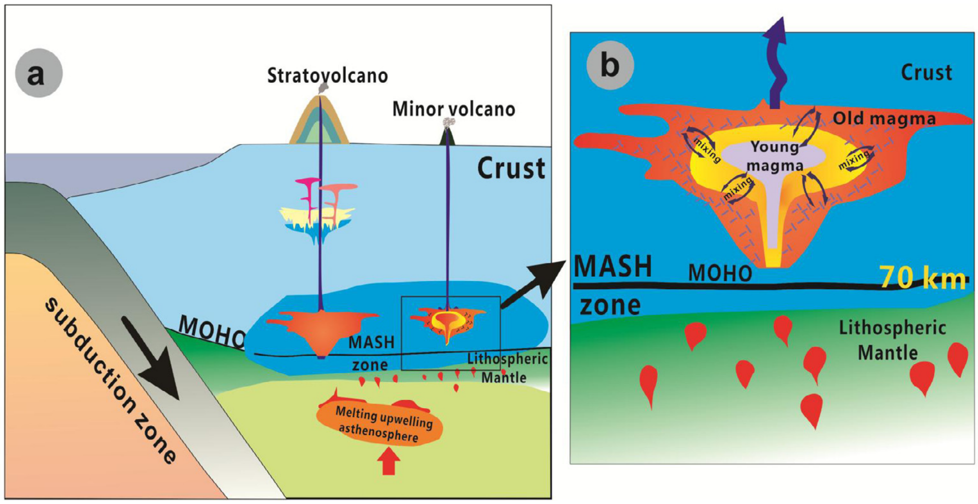

Fig. 7. Conceptual sketch of the large scale CVZ magmatic plumbing system at the base of the thickened continental crust. Melts from convective metasomatized sub-arc mantle ascends to a MASH zone at the MOHO (a). Lavas erupted from a stratovolcano may have experienced significant differentiation in both the MASH zone and en route to the Earth's surface, while those for some minor volcanos may preserve the deep crustal signatures such as high Sr/Y and Gd/Yb. U-series disequilibria of the Andagua lavas recorded the multiple emplacement sequences and mixing of magmas to the MASH zone which takes place within a few half-lives of ^{226}Ra (b).

Secondly, relatively high Rb/Cs of Quaternary lavas older than 30 Ma does not support a substantial contribution of sediments to the mantle wedge (Mamani et al., 2010); and thirdly, the aridity on the western Andean slope started from the latest Oligocene or Miocene (e.g. Dunai et al., 2005), suggesting that accumulation and delivery of sediments to the trench have been of minimal importance since ~30 Ma.

Although ^{238}U excess in the CVZ lavas could be inherited from the disequilibria signal from slab-derived fluid, the ^{230}Th excess and ^{231}Pa excesses clearly rule out such interpretation because Pa and Th are generally considered immobile in a fluid relative to U (Turner et al., 2003 and reference therein). The Sr isotope compositions of the Andagua lavas do not correlate with (^{238}U)/(^{232}Th) and U-series daughter-parent ratios (Fig. 8), indicating that the observed U-series disequilibria were not derived from slab-derived materials with high ^{87}Sr/^{86}Sr which is added to the mantle wedge. Therefore, we propose that U-series

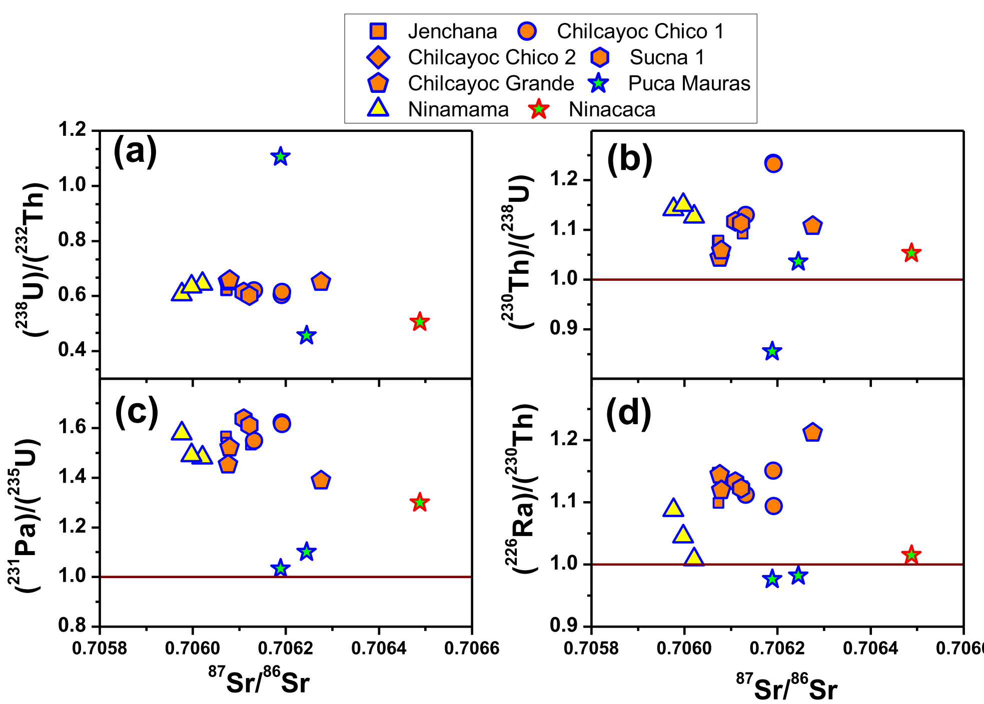

Fig. 8. Correlations of ^{87}Sr/^{86}Sr with U-series data. There is no correlation between ^{87}Sr/^{86}Sr and U-series disequilibria of the Andagua lavas, suggesting that the disequilibria cannot be due to heterogeneity in the mantle wedge.

disequilibria in Andagua lavas are better explained by partial melting of the mantle wedge in the garnet stability field as shown in a simplified in-growth melting model (Table 3 and Fig. 9). Based on different residence time of nuclides during mantle melting, in-growth melting models (such as fluxing melting, dynamic melting, and equilibrium porous flow) can reproduce the observed U-series disequilibria in subduction zone lavas with reasonable parameters applied including partition coefficients, porosity, and melting rate (e.g. Spiegelman and Elliott, 1993; Thomas et al., 2002; Turner et al., 2006; Huang et al., 2011). Because the rationale of the three in-growth melting models is similar in that highly incompatible U-series nuclides are fractionated from each other by mantle melting at low porosity of ∼1–2‰, this study just uses the equilibrium porous flow model as a representative because it is consistent with experimental constrains and thermal structure of melting process in the mantle wedge (see a recent summary in Huang et al. (2016)).

Here we use the equilibrium porous flow model of Spiegelman and Elliott (1993) to reproduce the U-Th-Pa-Ra disequilibrium observations. In-growth melting of the mantle wedge can explain the ^{231}Pa and ^{230}Th excesses in the Andagua lavas, while the ^{226}Ra excess may have in addition experienced ageing effect and it is therefore suggested that the time elapsed since generation of the disequilibrium is less than 8000 years. As subduction zone lavas are generally produced by mantle melting followed by magma differentiation in the crust (e.g. Gill, 1981), multiple U-series parent-daughter pairs with distinct temporal implications can constrain the time-scales of these two steps of magmatism. The in-growth model to produce ^{231}Pa excess requires that the time-scale for the mantle wedge melting was long enough to produce the observed disequilibrium which would be comparable to the half-life of ^{231}Pa (33 kyrs) (Huang et al., 2011, 2016), which is much longer than the half-live of ^{226}Ra, whereas magma differentiation in the crust must take less than 8000 years before eruption in order to preserve the produced ^{226}Ra excess.

Finally, (^{226}Ra)/(^{230}Th) of the Andagua lavas is positively correlated to Sr/Th and Ba/Th (Fig. 4f). Such correlations were previously explained as a signal of slab-derived fluid enriched in fluid-mobile elements (such as Sr, Ba, and Ra) relative to immobile elements (such as Th) (Turner et al., 2000). Because Ba/Th and Sr/Th dramatically decrease with increasing SiO_2 contents (Fig. 6), this more likely reflects magma mixing for the Andagua case, not the addition of slab fluids to the mantle source. Although

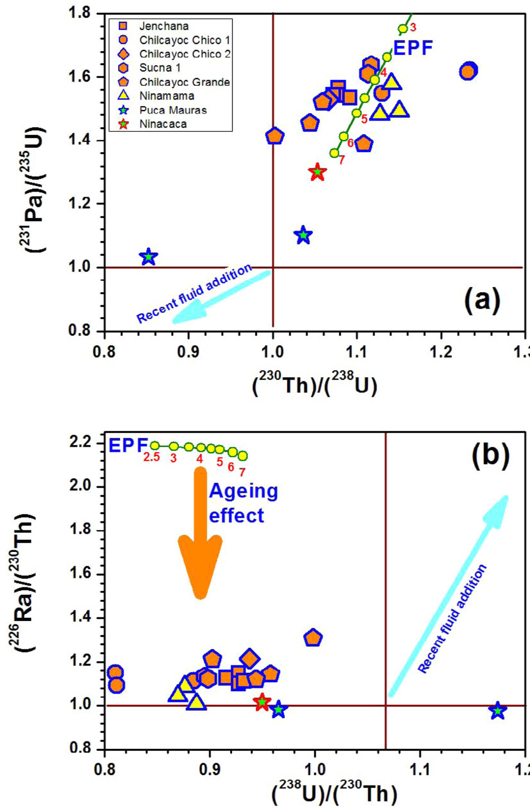

Fig. 9. An equilibrium porous flow (EPF) model is applied as a representative to simulate the correlations between (^{231}Pa)/(^{235}U) and (^{230}Th)/(^{238}U) (a) and between (^{226}Ra)/(^{230}Th) and (^{238}U)/(^{230}Th) (b). The equations are from Spiegelman and Elliott (1993) and Lundstrom (2003). Parameters used in the EPF model include: porosity, 0.002; melting degree, 15%; peridotite density, 3340 kg/m^3; melt density, 2800 kg/m^3; Partition coefficients of U-series nuclides between mantle minerals and melt are listed in Table 3. The numbers near the EPF model curve indicate melting rate with the unit of 10^{-4} kg m^{-3} yr^{-1}, within the normal range used in the literature (Bourdon and Sims, 2003; Turner et al., 2003). Recent addition of U and Ra-rich fluids would produce ^{238}U and ^{226}Ra excesses, not consistent with the data of Andagua lavas.

the initial (^{226}Ra)/(^{230}Th) of the Andagua lavas is not exactly known, also the positive correlation between (^{226}Ra)/(^{230}Th) and Sr/Th (Fig. 4f) can be explained by deep mixing between the felsic and mafic magma. Furthermore, as the negative correlation of SiO_2 with Ra/Th, Ba/Th, and Sr/Th are observed in other subduction zone lavas,

Table 3
Partition coefficients of U-series nuclides used in the EPF model in Fig. 9.

	Mode[1]	U	Th	Pa	Ra
$^{olivine/melt}D$[2]	52	6.0×10^{-5}	9.5×10^{-6}	6.0×10^{-8}	5.8×10^{-8}
$^{opx-melt}D$[2]	28	7.8×10^{-3}	3.0×10^{-3}	7.8×10^{-6}	6.0×10^{-7}
$^{cpx-melt}D$[2]	18	7.0×10^{-3}	6.0×10^{-3}	1.8×10^{-9}	4.1×10^{-6}
$^{garnet-melt}D$[2]	2	2.1×10^{-2}	6.0×10^{-3}	5.8×10^{-4}	7.0×10^{-9}

[1] Mineral modes are similar to those of fertile mantle in Turner et al. (2006).
[2] Partition coefficients of most nuclides are similar to the values used in Turner et al. (2006) based on the summary in Blundy and Wood (2003), while $^{cpx-melt}D_{U-Th}$ is from experiment TM1094-10 and $^{garnet-melt}D_{U-Th}$ from experiment Mo 895-2 in Salters and Longhi (1999).

such as South Lesser Antilles and South Chile (Sigmarsson et al., 2002; Huang et al., 2011), it is likely that magma evolution including mixing also plays a role in producing the correlations among Sr/Th, Ba/Th, and Ra/Th.

6. CONCLUSIONS

The Andagua trachyandesite lavas from southern Peru preserve information of magma differentiation in the lower continental crust, providing constraints on the process and time-scale of magma differentiation at the base of deep crust. Andagua lavas have ^{230}Th, ^{231}Pa, and ^{226}Ra excesses, except a few more differentiated samples that were likely affected by crystallizing accessory minerals (such as allanite, apatite, and zircon). Based on the correlations of U-series disequilibria with SiO_2 content and trace element ratios (such as Sr/Th and Gd/Yb), we argue that the Andagua lavas were produced by mixing of fresh mantle-derived magma with felsic melt of earlier emplaced basalts in the deep crust. Such differentiation processes should take place in the MASH zone where the magmas are stored warmly.

Because of a lack of sediment in the Chile-Peru trench, ^{230}Th and ^{231}Pa excesses in the Andagua lavas are best explained by in-growth melting of the mantle wedge. In-growth melting can also produce the ^{226}Ra excess observed in Andagua lavas. Collectively, U-series disequilibria in the Andagua lavas requires that the time-scales of mantle melting in the wedge should be at least comparable to the half-live of ^{231}Pa (33 kyrs), whereas the ^{226}Ra excess indicates that the time elapsed since magma emplacement and differentiation in the deep crust is within several thousand years.

ACKNOWLEDGEMENT

This work is supported by the National Science Foundation of China (41573017 and 41325011), the 111 project, the Fundamental Research Funds for the Central Universities, and Stake Key Laboratory of Isotope Geochemistry grants (SLKIG-KF-12-05, SKLIG-KF-13-03, SKLIG-JY-12-01 and SKLIG-JY-13-03). We appreciate the editorial handling by Anthony Dosseto and constructive comments from Lucy McGee and the other two anonymous reviewers. We also thank Yongli Xue and Juan Xu for collecting data and drafting some figures.

REFERENCES

Asmerom Y., DuFrane S. A., Mukasa S. B., Cheng H. and Edwards R. L. (2005) Time scale of magma differentiation in arcs from protactinium-radium isotopic data. *Geology* **33**, 633–636.

Avanzinelli R., Prytulak J., Skora S., Heumann A., Koetsier G. and Elliott T. (2012) Combined ^{238}U–^{230}Th and ^{235}U–^{231}Pa constraints on the transport of slab-derived material beneath the Mariana Islands. *Geochim. Cosmochim. Acta* **92**, 308–328.

Baby P., Rochat P., Mascle G. and Herail G. H. (1997) Neogene shortening contribution to crustal thickening in the back arc of the Central Andes. *Geology* **25**, 883–886.

Barboni M., Boehnke P., Schmitt A. K., Harrison T. M., Shane P., Bouvier A.-S. and Baumgartne L. (2016) Warm storage for arc magmas. *PNAS* **113**, 13959–13964.

Blundy J. and Wood B. (2003) Mineral-melt partitioning of Uranium, Thorium and their daughters. *Rev. Mineral. Geochem.* **52**, 59–123.

Bourdon B. and Sims K. (2003) U-series constraints on intraplate basaltic magmatism. *Rev. Mineral. Geochem.* **52**, 215–254.

Bourdon B., Turner S. and Allègre C. (1999) Melting dynamics beneath the Tonga-Kermadec island arc inferred from ^{231}Pa-^{235}U systematics. *Science* **286**, 2491–2493.

Bourdon B., Worner G. and Zindleer A. (2000) U-series evidence for crustal involvement and magma residence times in the petrogenesis of Parinacota volcano. *Chile. Contrib. Mineral Petrol.* **139**, 458–469.

Bourdon B., Turner S. and Dosseto A. (2003) Dehydration and partial melting in subduction zones: constrains from U-series disequilibria. *J. Geophys. Res.* **108**(B6), 2291.

Cabrera, M., and Thouret, J.-C. (2000) Volcanismo monogenetico en el Sur del Peru: Andaguay Huambo. X congreso Peruano de Geologia: Sociedad Geological del Peru, Resumens.

Caldas J. V. (1993) Geologia de los Cuadrangulas de Huambo y Orcopampa; Hojas 32-r & 31-r. *Boletin - Instituto Geologico Mineroy Metalurgico. Seria A: Carta Geologica National* **46**.

Davidson J. P. and de Silva S. L. (1992) Volcanic rocks from the Bolivian Altiplano: Insights into crustal structure, contamination, and magmagenesis in the Central Andes. *Geology* **20**, 1127–1130.

Delacour A., Gerbe M.-C., Thouret J.-C., Wörner G. and Paquereau-Lebti P. (2007) Magma evolution of Quaternary minor volcanic centres in southern Peru, Central Andes. *Bull. Volcanol.* **69**, 581–608.

Delph J. R., Ward K. M., Zandt G., Ducea M. N. and Beck S. L. (2017) Imaging a magma plumbing system from MASH zone to magma reservoir. *Earth Planet. Sci. Lett.* **457**, 313–324.

DePaolo D. J. (1981) Trace element and isotopic effects of combined wallrock assimilation and fractional crystallization. *Earth Planet. Sci. Lett.* **53**, 189–202.

Dosseto A., Bourdon B., Joron J.-L. and Dupré B. (2003) U-Th-Pa-Ra study of the Kamchatka arc: new constraints on the genesis of arc lavas. *Geochim. Cosmochim. Acta* **67**(15), 2857–2877.

Dufek J. and Cooper K. M. (2005) ^{226}Ra/^{230}Th excess generated in the lower crust: Implications for magma transport and storage time scales. *Geology* **37**, 833–836.

Dunai T. J., González G. and Juez-Larré J. (2005) Oligocene-Miocene age of aridity in the Atacama Desert revealed by exposure dating of erosion-sensitive landforms. *Geology* **33**, 321–324.

Gałaś A. (2011) The extent and volcanic structures of the Quaternary Andahua Group, Andes, southern Peru. *Ann. Soc. Geol. Pol.* **81**, 1–19.

Gałaś A. (2014) Petrology and new data on the geochemistry of the Andahua volcanic group (Central Andes, southern Peru). *J. S. Am. Earth Sci.* **56**, 301–315.

Garrison J., Davidson J., Reid M. and Turner S. (2006) Source versus differentiation controls on U-series disequilibria: insights from Cotopaxi Volcano, Ecuador. *Earth Planet. Sci. Lett.* **244**, 548–565.

George R., Turner S., Hawkesworth C., Morris J., Nye C., Ryan J. and Zheng S.-H. (2003) Melting processes and fluid and sediment transport rates along the Alaska-Aleutian arc from an integrated U-Th-Ra-Be isotope study. *J. Geophys. Res.* **108** (B5), 2252.

Gill J. B. (1981) *Orogenic Andesites and Plate Tectonics*. Springer-Verlag.

Grove T. and Kinzle R. (1986) Petrogenesis of andesites. *Ann. Rev. Earth Planet. Sci.* **14**, 417–454.

Harmon R. S., Barreiro B. A., Moorbath S., Hoefs J., Francis W., Thorpe R. S., Deruelle B., McHugh J. and Viglino J. A. (1984) Regional O-, Sr-, and Pb-isotope relationships in late Cenozoic calc-alkaline lavas of the Andean Cordillera. *J. Geol. Soc., London* **141**, 803–822.

Hermann J. (2002) Allanite: thorium and light rare earth element carrier in subducted crust. *Chem. Geol.* **192**, 289–306.

Hildreth W. and Moorbath S. (1988) Crustal contributions to arc magmatism in the Andes of Central Chile. *Contrib. Miner. Petrol.* **98**, 455–489.

Huang F. and Lundstrom C. C. (2007) Pa-231 excesses in arc volcanic rocks: constraint on melting rates at convergent margins. *Geology* **35**(11), 1007–1010.

Huang F., Gao L. and Lundstrom C. C. (2008) The effect of assimilation, fractional crystallization, and ageing on U-series disequilibria in subduction zone lavas. *Geochim. Cosmochim. Acta* **72**, 4136–4145.

Huang F., Lundstrom C. C., Sigurdsson H. and Zhang Z. F. (2011) U-series disequilibria in Kick'em Jenny submarine volcano lavas: a new view of time-scales of magmatism in convergent margins. *Geochim. Cosmochim. Acta* **75**(1), 195–212.

Huang F., Xu J. and Zhang J. L. (2016) U-series disequilibria in subduction zone lavas: inherited from subducted slabs or produced by mantle in-growth melting? *Chem. Geol.* **440**, 179–190.

Koornneef J. M., Stracke A., Aciego S., Reubi O. and Bourdon B. (2010) A new method for U-Th–Pa–Ra separation and accurate measurement of ^{234}U–^{230}Th–^{231}Pa–^{226}Ra disequilibria in volcanic rocks by MC-ICPMS. *Chem. Geol.* **277**, 30–41.

Lundstrom C. C. (2003) Uranium series disequilibria in mid-ocean ridge basalts: observations and models of basalt genesis. *Rev. Mineral. Geochem.* **52**, 175–214.

Mamani M., Wörner G. and Sempere T. (2010) Geochemical variations in igneous rocks of the Central Andean orocline (13 S to 18 S): tracing crustal thickening and magma generation through time and space. *GSA Bullet.* **122**, 162–182.

Mattioli M., Renzulli A., Menna M. and Holm P. (2006) Rapid ascent and contamination of magmas through the thick crust of the CVZ (Andes, Ollagüe region): Evidence from a nearly aphyric high-K andesite with skeletal olivines. *J. Volcanol. Geoth. Res.* **158**, 87–105.

Pertermann M., Hirschmann M. M., Hametner K., Günther D. and Schmidt M. W. (2004) Experimental determination of trace element partitioning between garnet and silica-rich liquid during anhydrous partial melting of MORB-like eclogite. *G-Cubed* **5**. http://dx.doi.org/10.1029/2003GC000638.

Pickett D. A. and Murrell M. T. (1997) Observation of ^{231}Pa/^{235}U disequilibrium in volcanic rocks. *Earth Planet. Sci. Lett.* **148**, 259–271.

Prowatke S. and Klemme S. (2006) Trace element partitioning between apatite and silicate melts. *Geochim. Cosmochim. Acta* **70**, 4513–4527.

Prytulak J., Elliott T., Hoffmann D. L. and Coath C. D. (2008) Assessment of USGS BCR-2 as a reference material for silicate rock U-Pa disequilibrium measurements. *Geostan. Geoanal. Res.* **32**, 55–63.

Reagan M. K., Turner S., Legg M., Sims K. W. W. and Hards L. (2008) ^{238}U- and ^{232}Th-decay series constraints on the time-scales of crystal fractionation to produce the phonolite erupted in 2004 near Tristan da Cunha, South Atlantic Ocean. *Geochim. Cosmochim. Acta* **73**, 4367–4378.

Regelous M., Turner S. P., Elliot T. R., Rostami K. and Hawkesworth C. J. (2004) Rapid measurement of femtogram quantities of protactinium in silicate rock samples by multicollector inductivyle coupled plasma-mass spectrometry. *Anal. Chem.* **76**, 3584–3589.

Reubi O., Bourdon B., Dungan M. A., Koornneef J. M., Sellés D., Langmuir C. H. and Aciego S. (2011) Assimilation of the plutonic roots of the Andean arc controls variations in U-series disequilibria at Volcan Llaima, Chile. *Earth Planet. Sci. Lett.* **303**, 37–47.

Reubi O., Sims K. W. W. and Bourdon B. (2014) ^{238}U–^{230}Th equilibrium in arc magmas and implications for the time scales of mantle metasomatism. *Earth Planet. Sci. Lett.* **391**, 146–158.

Sørensen E. V. and Holm M. (2008) Petrological inferences on the evolution of magmas erupted in the Andagua Valley, Peru (Central Volcanic Zone). *J. Volcanol. Geoth. Res.* **177**, 378–396.

Salters J. M. and Longhi J. (1999) Trace element partitioning during the initial stages of melting beneath mid-ocean ridges. *Earth Planet. Sci. Lett.* **166**, 15–30.

Sigmarsson O., Chmeleff J., Morris J. and Lopez-Escobar L. (2002) Origin of ^{226}Ra-^{230}Th disequilibria in arc lavas from southern Chile and implications for magma transfer time. *Earth Planet. Sci. Lett.* **196**, 189–196.

Sims K. W. W., Gill J. B., Dosseto A., Hoffmann D. L., Lundstrom C. C., Williams R. W., Ball L., Tollstrup D., Turner S., Prytulak J., Glessner J. J. G., Standish J. J. and Elliott T. (2008) An inter-laboratory assessment of the thorium isotopic composition of synthetic and rock reference materials. *Geostan. Geoanal. Res.* **32**, 65–91.

Spiegelman M. and Elliott T. (1993) Consequences of melt transport for uranium series disequilibrium in young lavas. *Earth Planet. Sci. Lett.* **118**, 1–20.

Stern C. R. (2004) Active Andean volcanism: its geologic and tectonic setting. *Revista Geológica de Chile* **31**, 161–206.

Thomas R. B., Hirschmann M. M., Cheng H., Reagan M. K. and Edwards R. L. (2002) (^{231}Pa/^{235}U)-(^{230}Th/^{238}U) of young mafic volcanic rocks from Nicaragua and Costa Rica and the influence of flux melting on U-series systematics of arc lavas. *Geochim. Cosmochim. Acta* **66**(24), 4287–4309.

Thornburg T. M. and Kulm L. D. (1987) Sedimentation in the Chile Trench: depositional morphologies, lithofacies, and stratigraphy. *Geol. Soc. Am. Bull.* **98**, 33–52.

Turner S., Bourdon B., Hawkesworth C. and Evans P. (2000) ^{226}Ra-^{230}Th evidence for multiple dehydration events, rapid melt ascent and the time scales of differentiation beneath the Tonga-Kermadec island arc. *Earth Planet. Sci. Lett.* **179**, 581–593.

Turner S., Evans P. and Hawkesworth C. (2001) Ultrafast source-to-surface movement of melt at island arcs from ^{226}Ra-^{230}Th systematics. *Science* **292**, 1363–1366.

Turner S., Bourdon B. and Gill J. (2003) U-Series isotopes and magma genesis at convergent margins. *Rev. Mineral. Geochem.* **52**, 255–315.

Turner S., Regelous M., Hawkesworth C. and Rostami K. (2006) Partial melting processes above subducting plates: constraints from ^{231}Pa-^{235}U disequilibria. *Geochim. Cosmochim. Acta* **70**, 480–503.

Yuan X., Sobolev S. V. and Kind R. (2002) Moho topography in the Central Andes and its geodynamic implications. *Earth Planet. Sci. Lett.* **199**, 389–402.

Zajacz Z. and Halter W. (2007) LA-ICPMS analyses of silicate melt inclusions in co-precipitated minerals: Quantification, data analysis and mineral/melt partitioning. *Geochim. Cosmochim. Acta* **71**, 1021–1040.

Zellmer G. F., Hawkesworth C. J., Sparks R. S. J., Thomas L. E., Harford C. L., Brewer T. S. and Loughlin S. C. (2003) Geochemical evolution of the Soufriere Hills volcano, Montserrat, Lesser Antilles volcanic arc. *J. Petrol.* **44**, 1349–1374.

Associate editor: Anthony Dosseto